ACS APPLIED MATERIALS & INTERFACES

Forum Article

www.acsami.org

Binary Polymer Brushes of Strongly Immiscible Polymers

Elza Chu, Tashnia Babar, Michael F. Bruist, and Alexander Sidorenko*

Department of Chemistry & Biochemistry, University of the Sciences, Philadelphia, Pennsylvania 19104, United States

ABSTRACT: The phenomenon of microphase separation is an example of self-assembly in soft matter and has been observed in block copolymers (BCPs) and similar materials (i.e., supramolecular assemblies (SMAs) and homo/block copolymer blends (HBCs)). In this study, we use microphase separation to construct responsive polymer brushes that collapse to generate periodic surfaces. This is achieved by a chemical reaction between the minor block (10%, poly(4-vinylpyridine)) of the block copolymer and a substrate. The major block of polystyrene (PS) forms mosaic-like arrays of grafted patches that are 10−20 nm in size. Depending on the nature of the assembly (SMA, HBC, or neat BCP) and annealing method (exposure to vapors of different solvents or heating above the glass transition temperature), a range of "mosaic" brushes with different parameters can be obtained. Successive grafting of a secondary polymer (polyacrylamide, PAAm) results in the fabrication of binary polymer brushes (BPBs). Upon being exposed to specific selective solvents, BPBs may adopt different conformations. The surface tension and adhesion of the binary brush are governed by the polymer occupying the top stratum. The "mosaic" brush approach allows for a combination of strongly immiscible polymers in one brush. This facilitates substantial contrast in the surface properties upon switching, previously only possible for substrates composed of predetermined nanostructures. We also demonstrate a possible application of such PS/PAAm brushes in a tunable bioadhesion−bioadhesive (PS on top) or nonbioadhesive (PAAm on top) surface as revealed by *Escherichia coli* bacterial seeding.

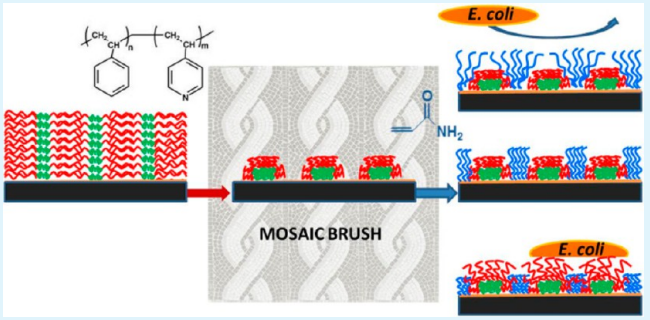

KEYWORDS: *binary polymer brush, grafting through, block copolymer, responsive brush, supramolecular assembly, bioadhesion*

INTRODUCTION

Dynamic control or manipulation of surfaces and interphases is a very attractive concept that has strong potential for involvement in upcoming technologies.[1−5] By dynamic control, we mean reversible changes in surface properties during operation (i.e., in situ). This concept can be realized by the presence of two (or more) different components that are readily available to cover the top stratum. In such systems, surface properties are dominated by the component that is on top, whereas the other component remains hidden and collapsed, and vice versa. The most prominent contrast and most dramatic response can be achieved by combining components with distinctly different properties. A model system composed of two diverse components has demonstrated the full potential of this approach: hydrophobic nanoposts embedded in a hydrogel revealed an ideal wetting response from superhydrophobic to superhydrophilic.[1,2] Previously, such extremely opposing responses could only be constructed on inorganic substrates prefabricated with nanostructures.[1,2] Hence, the combination of physical roughness from the nanostructures in conjunction with hydrophilic polymer brushes produced the observed effects.

A more practical approach to the same concept is based on binary polymer brushes (BPB).[3] A BPB is a dense monolayer of two types of permanently attached polymer coils. Upon being exposed to a common solvent (i.e., nonselective and good), both components are present at the surface and collectively govern the system's interfacial properties (Figure 1, state "c"). However, when a selective solvent good for polymer A is used, the solvent interactions push chains of A to occupy the surface while chains of B collapse. Upon drying, the microphase separation in BPB is preserved, and component A dominates the properties of the surface (Figure 1, path "c" to "a"). The situation is reversed if a selective solvent good for polymer B is used (Figure 1, path "c" to "b"). If the top component forms a layer of entangled coils, a direct switch ("a" to "b") is hindered. In a selective solvent good for B, the surface-dominating layer of A is in a glassy state and remains on top. Even if the "B"-selective solvent can penetrate through component A, its glassy conformation restricts component B to the bottom stratum.[6]

The widely adopted synthesis of BPBs involves a two-step grafting process: grafting of polymer A followed by grafting of polymer B. The grafting approaches commonly used are "grafting from",[3,6] "grafting to",[7,8] and a combination of both. The key component of this strategy is the common solvent. It facilitates grafting of polymer B while the already grafted A is swollen, and therefore allows access of monomers or chains of

Special Issue: Forum on Polymeric Nanostructures: Recent Advances toward Applications

Received: November 16, 2014
Accepted: January 29, 2015
Published: February 10, 2015

DOI: 10.1021/am5080248
ACS Appl. Mater. Interfaces 2015, 7, 12505−12515

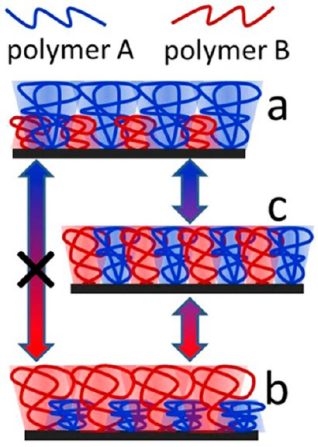

Figure 1. Principles of the response of binary polymer brushes to external stimuli. A monolayer of two kinds of polymer chains (A and B) attached concurrently to a substrate demonstrates microphase lateral (state "c", common solvent) and normal separation (state "a" after exposure to selective solvent good for polymer A, and state "b" after exposure to a selective solvent good for B). Direct transition from "a" to "b", and vice versa, is hindered by the polymer occupying the top stratum.

B to reactive sites on the substrate surface. A common solvent is also required for surface conversion to state "c" and to enable switching between states "a" and "b". However, the scarcity of common solvents for pairs of different polymers restricts the diversity of such BPBs. Consequently, previously constructed BPBs do not demonstrate the wide range of responses observed in systems composed of inorganic nanostructures.[1−5] This is particularly true if a BPB with a strong contrast in switching is to be devised (e.g., polar and nonpolar). For simplicity, we will call polymers with no common solvents "strongly immiscible polymers". This dilemma was the impetus for the research that we report in this paper.

Previous publications have demonstrated microphase separation in BPBs. Lateral structures ("dimples" and "ripples") form simultaneously with orthogonal separation (top and bottom strata) as a result of the interplay between the solvent and polymers.[9,10] The lateral separation is stable and occurs on the scale of an extended chain length (i.e., ∼100 nm). The phenomenon of microphase separation was first discovered in block copolymers.[11,12] Recent advances in thin films of block copolymer supramolecular assemblies (SMAs)[13,14] and block/homopolymer blends[15,16] inspired the idea to integrate the BPB and SMA platforms.

Thin films of SMAs composed of a block copolymer and a small molecule additive reveal well-defined microphase separation. The additives are selectively coupled with monomers of one of the blocks by hydrogen bonding[13,14,17,18] or other weaker interactions.[19,20] The annealing of SMAs allows for the formation of a number of stable morphologies, including densely packed spheres, hexagonally ordered cylinders, bicontinuous gyroids, and lamellas. The SMA films can be easily converted to porous structures by removing the additives with a selective solvent. Depending on the morphology and orientation (parallel vs perpendicular) of the SMAs on the substrate, several distinct patterns have been observed, such as hexagonally packed wells and parallel trenches (fingerprint-like pattern). The typical size and periodicity of these features vary in the range of 10−50 nm. Similarly, the addition of a homopolymer component identical to one of the blocks is another option to alter the morphology of the original block copolymer. If the homopolymer matches the minor block, it is solubilized in the domains. This increases the size of the domain and eventually alters the morphology of the homo/block copolymer blend (HBC).[15,21−24] On the contrary, if the homopolymer is identical to the major block, it increases the neighbor-to-neighbor distance (periodicity) of the formed periodic structure of the BPB.[25]

In this work, we fabricate a nanopatterned surface using SMA or HBC thin films to obtain a responsive polymer brush with a well-defined morphology (as well as can be achieved using microphase separation). The first step is synthesis of a "mosaic" polymer brush obtained by grafting a block copolymer to the substrate surface. This is accomplished by the deposition of SMA or HBC thin films composed of a minor block (poly(4-vinylpyridine), P4VP) capable of chemical binding to reactive sites on the substrate surface (Figure 2). After the removal of additives and unreacted polymers with a good solvent, collapsing the grafted polymer with a selective nonsolvent reveals patches of the grafted polymer polystyrene (PS), which are similar in appearance to ancient mosaic tiles. Hence, we

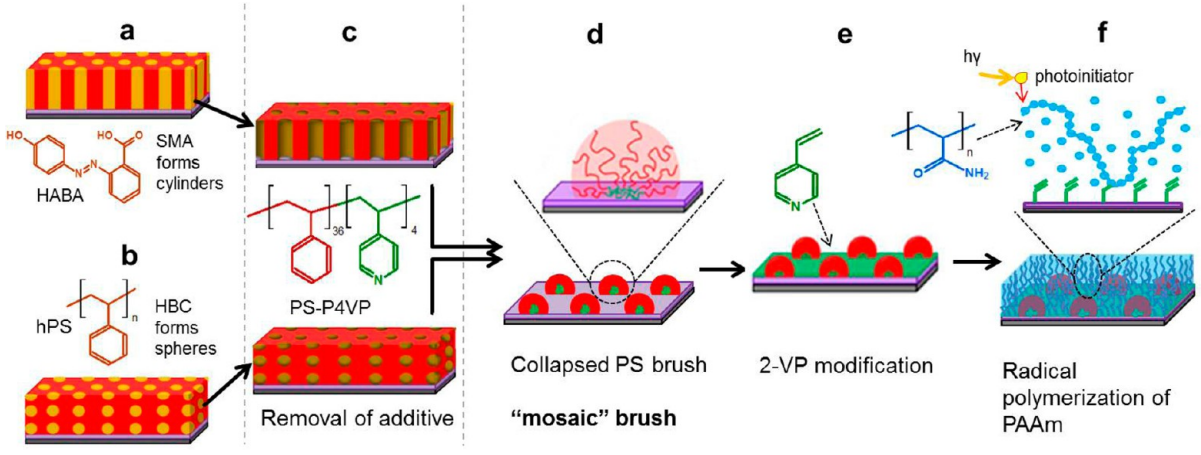

Figure 2. Formation of a BCP assembly (SMA or HBC) with PS−P4VP and an additive (HABA or hPS) via the "grafting to" method (a, b), removal of additive (c), collapse of PS to form a "mosaic" brush (d), 2VP-modification of interlaced surface (e), and "grafting through" of PAAm to form the BPB (f).

DOI: 10.1021/am5080248
ACS Appl. Mater. Interfaces 2015, 7, 12505−12515

refer to such brush templates as "mosaic" brushes. With regard to strongly immiscible polymer pairs (no common solvents), such techniques that utilize presegregated domains can be used to build BPBs with more dissimilar response changes.

The second step consists of grafting a complementary polymer to the available reactive sites (the free surface of PS). Even though "grafting to" and "grafting from" techniques are equally available for secondary modifications, we found it particularly suitable to use a "grafting through" approach. This "mosaic" hybrid approach allows for the introduction of two strongly immiscible polymers, polar polyacrylamide (PAAm) and nonpolar polystyrene (PS), with contrasting properties. The sequence is presented in Figure 2.

EXPERIMENTAL SECTION

Materials. (p-Bromophenyl)trimethoxysilane (Gelest, Inc.) and poly(styrene-*b*-4-vinylpyridine) (M_n: PS (35500 g mol^{-1}), P4VP (4400 g mol^{-1}), M_w/M_n = 1.09 for both blocks, PS−P4VP, purchased from Polymer Source, Inc.) were used as received. 2-(4-hydroxyphenylazo)benzoic acid (HABA), homopolymer polystyrene (hPS, M_n: 140 kDa, M_w: 230 kDa), triethylamine (TEA), acrylamide (AAm), 2-hydroxy-4′-(2-hydroxyethoxy)-2-methyl-propiophenone (photoinitiator, PI), toluene, methanol (MeOH), 1,4-dioxane, chloroform, and tetrahydrofuran (THF) were purchased from Sigma-Aldrich. 2-Vinylpyridine (2VP, Aldrich) was purified through a p-*tert*-butylcatechol inhibitor remover column (Aldrich). All solvents were HPLC grade and used with no further purification. Deionized (DI) water was prepared using a Milli-Q50 Ultra Pure water system. Silicon (Si) wafers ((100) orientation, Addison Engineering) were cut to size and successively washed in ultrasonic baths of dichloromethane (Pharmco-AAPER), methanol, and DI water for 15 min each. The Si samples were then immersed in a 1:1:2 "alkali piranha" solution comprised of hydrogen peroxide (30 wt %, Aldrich), ammonium hydroxide (35 wt %, Pharmco), and DI water at 82 °C for 45 min. They were then thoroughly rinsed with DI water and blown dry with argon gas prior to use.

Synthesis. Si wafers were silanized in a 1% solution of (*p*-bromophenyl)trimethoxysilane (Br-silane) in toluene overnight to form a uniform self-assembled monolayer (SAM). The samples were rinsed in neat toluene and dried under argon gas. The layers of the SAM were flat and featureless as observed by atomic force microscopy (AFM). The thickness was 1.1 nm as measured by ellipsometry, assuming the refractive index of Br-silane n = 1.5 consistent with a close-packed layer. The samples with the SAM were dip-coated (~80 nm thick films) in 2% PS−P4VP in 1,4-dioxane solution with no additives, SMA with HABA (equimolar (1:1) to P4VP monomers),[13] or HBC with varying ratios of hPS to PS−P4VP (1:3, 1:1, and 3:1) in 1,4-dioxane. The films ranged from 70 to 90 nm. The films were vapor annealed in 1,4-dioxane (15 min), toluene (15 min), chloroform (5 min), or oven-annealed at 120 °C (4 days) to facilitate grafting of PS−P4VP. The HABA SMA samples were washed with MeOH to remove excess HABA prior to being rinsed with THF to remove ungrafted PS−P4VP and hPS as done for other samples. The grafted PS−P4VP samples were immersed in a THF:MeOH binary solvent to form clusters of PS (i.e., a "mosaic" brush).

"Mosaic" samples prepared as such were immersed overnight in 10% 2VP in chloroform with a catalytic amount of triethylamine to incorporate C═C bonds via a quaternization reaction between tertiary amine (2VP) and halogen (Br of the SAM). The samples were rinsed with chloroform and re-exposed to THF:MeOH binary solvent to ensure complete collapse of the PS-block. The "grafting through" of polyacrylamide (PAAm) between the PS−P4VP clusters was achieved via photoinitiated polymerization as follows. The C═C bond-modified surface was submerged in filtered 20% aqueous AAm solution with 1% PI, covered with a glass coverslip, and exposed to ultraviolet light (mercury "BlakRay" lamp, 100 W, 90 cm distance) for 30 min.[26] Excess unattached PAAm was removed via soaking and extensive rinses with DI water. Thorough removal of unattached polymers was facilitated by washing the PS−P4VP/PAAm samples successively with DI water, MeOH, toluene, and vice versa, three times. The samples were then blown dry with argon gas.

Characterization. Routine thickness measurements of the PS−P4VP/PAAm samples were taken using a custom lab-built manual null ellipsometer. The ellipsometer setup was comprised of a Helium−Neon laser (λ = 632.8 nm, Thor Laboratories) light source−polarizer−compensator−sample−analyzer−detector setup with a fixed angle of incidence at 70° as described by Motschmann et al.[27] Interpretation of the ellipsometric data was conducted as previously reported.[3]

Block copolymer and mosaic morphology AFM images were obtained using a diInnova (Veeco Metrology) scanning probe microscope in tapping mode. The AFM probes purchased from Budget Sensors and NT-MDT had resonant frequencies of 160−180 kHz and 87−230 kHz and spring constants of 48 N/m and 1.45−15.1 N/m, respectively. Force−distance measurements were performed using the diInnova AFM in contact mode. Gold-coated NT-MDT Etalon probes with a resonance frequency (±10%) and spring constant (±20%) of 77 kHz and 3.4 N/m were used. A series of 240 force−distance point measurements were taken successively for each dominating polymer (PS and PAAm) under water. All AFM images were treated and analyzed using WSxM software by Nanotec Electronica.[28]

The effect of a fraction of PS−P4VP/PAAm on the efficiency of BPB response to solvent changes was also observed using sessile droplet contact angle (CA) measurements from a custom-built apparatus.

Bioadhesion Studies. On the basis of research by Cunliffe et al.,[29] we analyzed the physical adhesion properties of *Escherichia coli* as they apply to switchable brushes. Using standard microbiological methods, *E. coli* was grown to an OD_{600} /mL of 0.8 (6.4×10^8 cells/mL) in 2XYT media (16 g/L tryptone, 10 g/L yeast extract, 5 g/L NaCl; Sigma). A sample of a PS−P4VP/PAAm brush was split in two halves, and each half had either PS or PAAm on top. The *E. coli* culture (5 mL dispersion) was added to a 6 cm Petri dish with the samples and incubated at 37 °C for 2 h in humid conditions. Unattached cells were removed by rinsing the samples with DI water. The distribution of attached *E. coli* was pictured by optical microscope images of air-dried samples. AFM revealed fine features of the cells.

RESULTS AND DISCUSSION

Synthesis and Characterization of PS−P4VP "Mosaic" Brush. We fabricated a novel PS−P4VP "mosaic" brush (Figure 2) and studied the effects of its morphology on grafting of the complementary polymer PAAm. The precursor BCP used in this study is a diblock of PS (M_n: 36000 g mol^{-1}) and P4VP (M_n: 3600 g mol^{-1}). Spherical morphology (body-centered cubic) is characteristic for such an asymmetric BCP with a 10% volume fraction of the minor block.[11] However, addition of an equimolar amount (with respect to the P4VP units of the minor block) of HABA increases the fraction of the P4VP+HABA block in the SMA to 24.3% volume[13,14] The SMA then adopts a new morphology—hexagonally packed cylinders. The perpendicular orientation of the cylinders as deposited is an essential feature of thin films of SMA (20−80 nm thickness). The hexagonal packing can be improved upon vapor annealing in 1,4-dioxane. Moreover, vapor annealing in chloroform alters the orientation of the cylinders from perpendicular to parallel with respect to the substrate surface. Extraction of HABA from the SMA films by a selective solvent (methanol) exposes nanoscopic-sized pores. This makes AFM characterization of the film morphology straightforward: the perpendicular cylinders of P4VP+HABA domains are seen as wells (occasionally in good hexagonal order), whereas the parallel cylinders leave grooves or short trenches. The periodicity of neat BCPs is observed to be 18 nm by AFM of thin films, and it increases up to 24.5 nm due to the presence of

DOI: 10.1021/am5080248
ACS Appl. Mater. Interfaces 2015, 7, 12505−12515

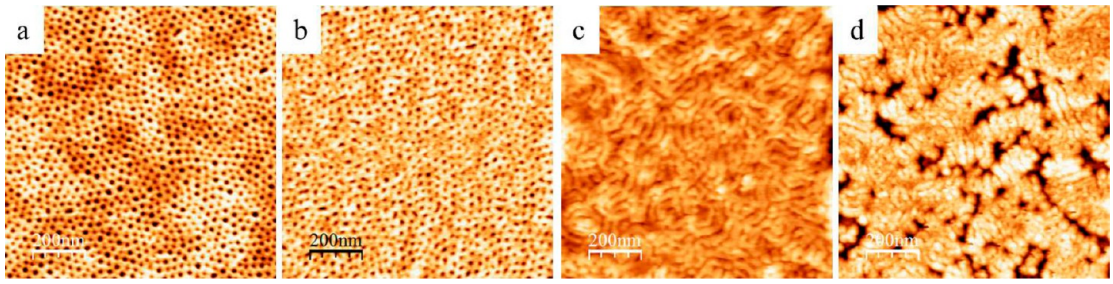

Figure 3. AFM topography of 1 μm × 1 μm thin films of SMAs after extraction of HABA with methanol: (a) no annealing, (b) upon vapor annealing in 1,4-dioxane, (c) upon vapor annealing in chloroform, and (d) upon thermal annealing at 120 °C. All images are ~10 nm in height.

Table 1. Grafting Amounts (Γ) of PS and PAAm (As Measured by Ellipsometry), Average Heights of Collapsed "Mosaic Tiles" (h_m), "Mosaic" Covered Surface Fractions (φ_m), and Contact Angles (θ) of BPBs with Various Solvents

assembly	solvent	h_m (nm)	Γ_{PS} (mg/m^2)*	Γ_{PAAm} (mg/m^2)*	φ_m	θ_{H_2O} (degrees)	θ_{MeOH} (degrees)	θ_{tol} (degrees)
PS−P4VP	1,4-dioxane	5.89	2.70	5.55	0.58	25.6 ± 1.4	26.3 ± 0.9	65.9 ± 4.2
	chloroform	5.11	3.00	3.58	0.59	25.4 ± 0.3	27.5 ± 1.8	67.7 ± 2.5
	toluene	6.92	2.65	6.32	0.56	25.6 ± 0.4	25.9 ± 0.2	68.2 ± 0.9
	Δ (thermal)	5.67	2.09	4.49	0.57	26.4 ± 0.3	27.0 ± 2.1	64.8 ± 0.8
SMA	1,4-dioxane	6.18	3.48	7.52	0.69	25.7 ± 3.6	34.7 ± 6.1	60.7 ± 2.0
	chloroform	6.46	2.65	9.89	0.57	24.7 ± 2.3	26.6 ± 1.7	28.9 ± 3.2
	toluene	6.56	2.53	7.98	0.56	23.0 ± 1.2	25.2 ± 0.6	33.2 ± 1.0
	Δ (thermal)	4.89	2.21	5.85	0.64	22.1 ± 0.4	26.3 ± 1.0	65.9 ± 3.6
HBC 25% hPS	1,4-dioxane	9.09	2.79	14.75	0.27	23.1 ± 0.1	26.0 ± 0.9	53.1 ± 4.0
	chloroform	6.38	2.25	7.94	0.56	27.0 ± 0.8	30.1 ± 4.3	79.7 ± 1.0
	toluene	4.95	1.57	9.83	0.34	26.7 ± 0.9	42.8 ± 0.8	73.3 ± 0.2
	Δ (thermal)	11.11	2.72	5.26	0.68	44.0 ± 3.5	56.7 ± 2.9	82.8 ± 1.5

*Grafting amount (Γ) is measured by ellipsometry as the thickness of the polymer layers assuming n = 1.59. The thickness value is converted to grafting amount as shown in the Experimental Section/ellipsometry.

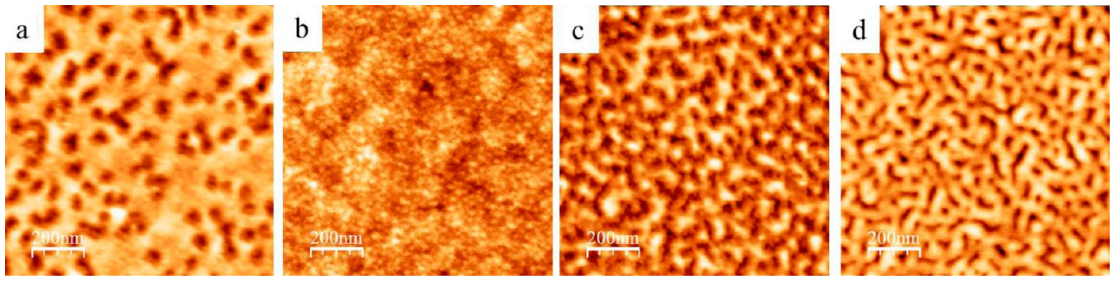

Figure 4. AFM topography of 1 μm × 1 μm grafted PS−P4VP after removal of ungrafted species for samples of (a) neat BCPs thermal annealed, (b) SMA annealed in 1,4-dioxane, (c) SMA annealed in toluene, and (d) HBC 25% hPS annealed in toluene.

HABA as it corresponds to perpendicular cylinders.[13] Previous studies have shown that thin films of PS−P4VP and corresponding SMAs with HABA adopt morphologies where the polar domains of P4VP (or P4VP+HABA) occupy the interface with the substrate.[14]

The addition of HABA increases the footprint of the P4VP domains relative to neat BCPs. Therefore, grafting of PS−P4VP from SMA may result in the local density of the "mosaic" brush being decreased relative to the "mosaic" prepared from neat BCPs. In the case of HBC, the addition of hPS should increase the interdomain distance without significant changes to the local grafting density. In other words, compact, taller "mosaic tiles" separated by larger distances would be expected compared to those of the SMA. In the latter scenario, we assume that P4VP domains are in contact with the substrate surface and are thus available for chemical reaction with the SAM, similar to the SMA.

We deposited thin films of neat BCPs and corresponding assemblies (PS−P4VP+HABA and PS−P4VP+hPS) on bromine-terminated SAMs and expected that grafting of the PS block would occur via quaternization reactions between pyridine species of the P4VP block and the bromine function of the SAM. To facilitate both microphase separation and chemical grafting, the films were annealed by either thermal annealing at 120 °C (above T_g) or solvent annealing.

The removal of HABA with methanol produced a range of SMA morphologies as shown in Figure 3. The SMA without annealing (Figure 3a) and upon annealing in vapors of 1,4-dioxane (Figure 3b) reveal wells reminiscent of perpendicular cylinders, whereas vapor annealing in chloroform and thermal annealing in a 120 °C oven form SMAs with parallel cylinder morphology that leave curved trenches (Figure 3c,d). Rinsing the PS−P4VP films (no additive and hPS) with methanol does not affect the surface characteristics.

DOI: 10.1021/am5080248
ACS Appl. Mater. Interfaces 2015, 7, 12505−12515

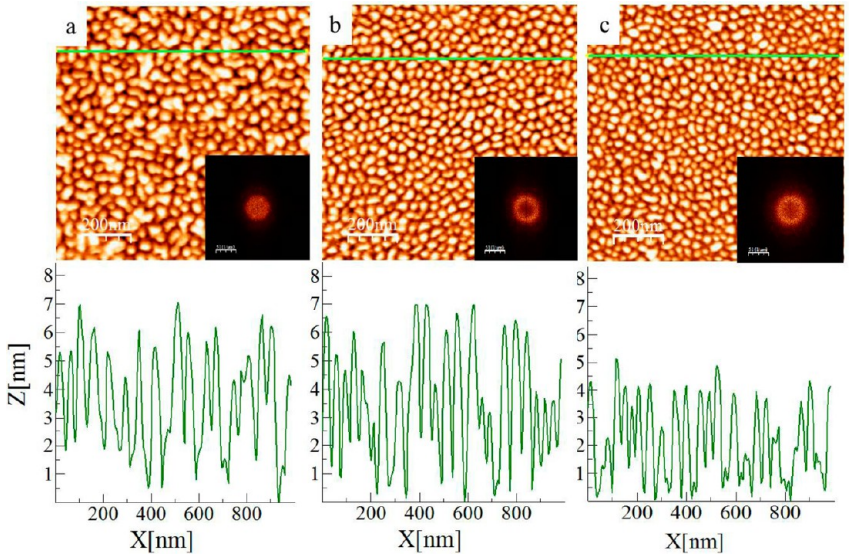

Figure 5. AFM topography of 1 μm × 1 μm area with attached FFT and height profiles for PS−P4VP "mosaic" brushes fabricated using HABA as an additive and vapor annealed with 1,4-dioxane (a), chloroform (b), and at 120 °C (c).

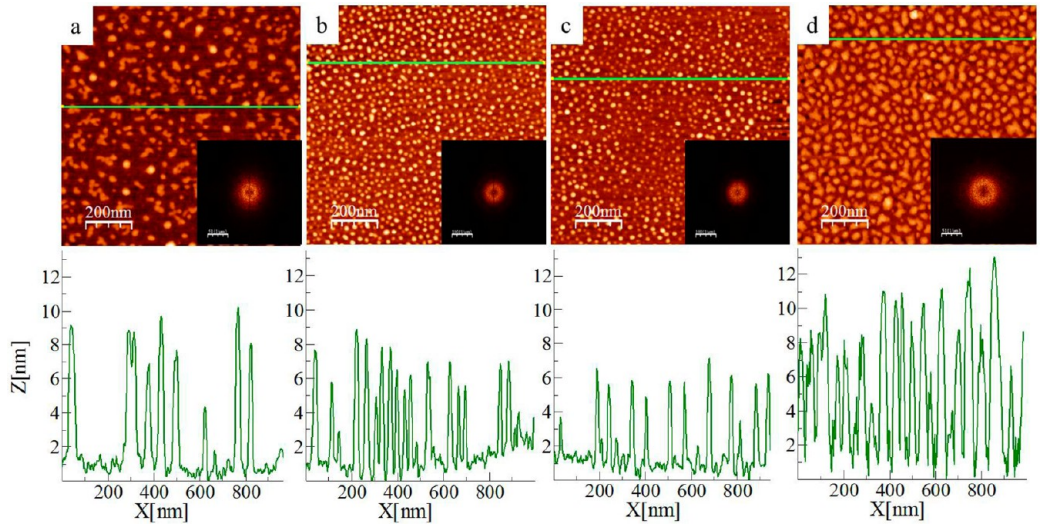

Figure 6. AFM topography of a 1 μm × 1 μm area with attached FFT and height profiles for PS−P4VP "mosaic" brushes fabricated with HBCs and vapor annealed with 1,4-dioxane (a), chloroform (b), toluene(c), and at 120 °C (d).

Upon the removal of any ungrafted polymers and additives with THF, we obtained a series of grafted PS−P4VP brushes. The thicknesses of the brushes varies between 2.5 and 3.5 mg/m^2 for vapor annealed samples (Table 1). In all cases, AFM reveals a number of fine textures; the most common are isolated islands (Figure 4a, neat BCPs), a flat brush that covers the entire surface with small bumps corresponding to P4VP-rich domains (Figure 4b, SMA upon 1,4-dioxane vapor annealing), percolating islands (Figure 4c, SMA upon toluene annealing), and a web-like texture with elongated features (Figure 4d, HBC upon toluene annealing).

The textures of grafted BCPs after mixing with a good solvent (THF, Figure 4) reflect the morphologies of overlapping/entangled polymer coils occupying the surface. The coils must be collapsed to reveal fine features of the grafted BCPs. However, direct exposure of the grafted BCPs to a weak solvent (e.g., methanol) has no effect because the BCPs are already in a glassy state, which hinders conformational changes. Therefore, to fully collapse the grafted BCP, we exposed the samples to a sequence of THF → THF−methanol binary solvent → methanol for 1 min each and then dried them only after the final methanol wash. This procedure allowed us to obtain well-defined "mosaic" brushes (i.e., grafted BCPs in a collapsed conformation composed of uniformly distributed features ("tiles") of the same height and similar volumes (Figures 5 and 6)). The "mosaic" brushes are consistent and uniform over the entire 12 × 12 mm^2 sample area.

The "mosaic" brushes formed using neat BCPs (no additives) as a reference did not demonstrate any variations regardless of the annealing method used. Figure 5 is a gallery of representative AFM topography images of "mosaic" brushes prepared from SMAs of PS−P4VP+HABA that were composed to study the effect of annealing methods on the morphology of the "mosaic". The corresponding profiles shown at the bottom reveal fairly uniform heights of the polymer tiles. Surface analyses using WSxM/Flooding applied to a 1 μm × 1 μm area produce average heights (shown in Table 1) and standard deviations. If vapor annealing is used, only small solvent-

DOI: 10.1021/am5080248
ACS Appl. Mater. Interfaces 2015, 7, 12505−12515

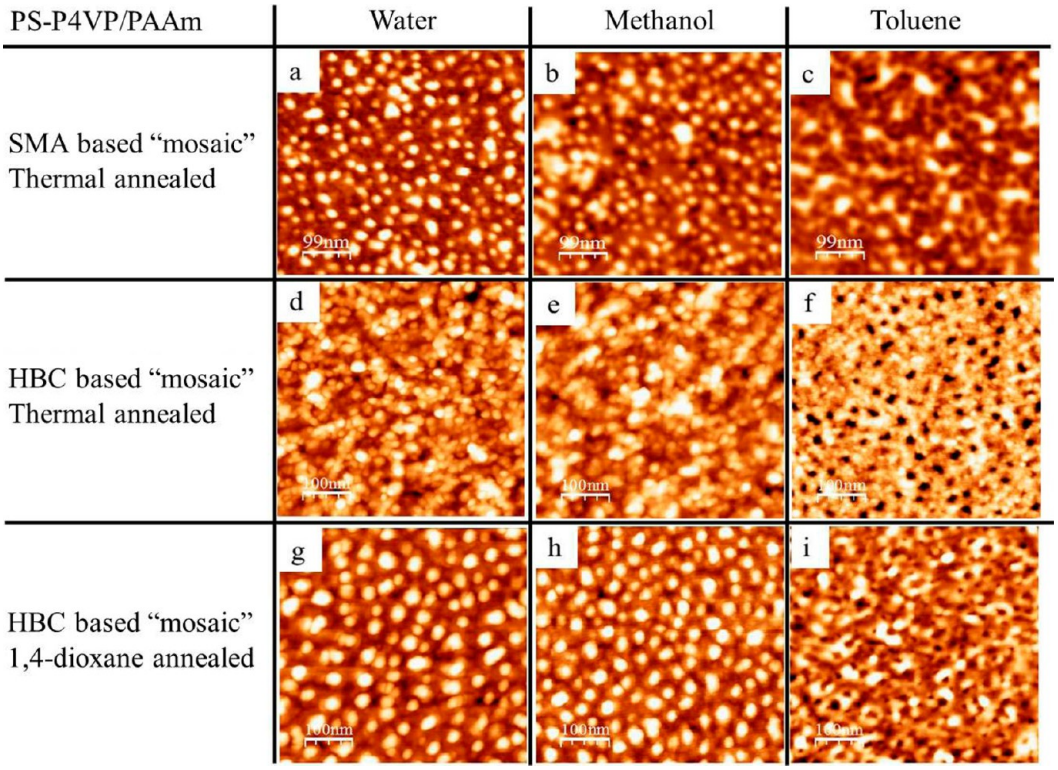

Figure 7. Changes in morphology observed in 0.5 μm × 0.5 μm AFM topography images for PS−P4VP/PAAm samples fabricated with thermally annealed SMA (a−c), HBC made with 25% hPS that is thermally annealed (d−f), and 1,4-dioxane annealed (g−i) samples exposed to water (a, d, and g), methanol (b, e, and h), and toluene (c, f, and i).

dependent variations in heights (ranging between 6.2 and 6.6 nm) are observed. Thermal annealing yields slightly lower heights. In all cases, the standard deviation of the tile heights does not exceed 0.6 nm. The embedded FFT images in Figure 5 are obtained from the corresponding topography scans. The clearly seen halos (diffuse rings) indicate a rather narrow distribution in lateral size and neighbor-to-neighbor distance (D) of the features. In all cases, the D values are about 60% larger than the interdomain distance of the SMAs with perpendicular cylinders. This means that only 40% of the P4VP+HABA domains are involved in grafting, thus the fading patterns (hexagonal or fingerprint-like) inferred by the SMAs.

In the case of HBC, the distance between P4VP domains increases due to hPS dispersed in the matrix. As suggested earlier, the use of HBC should result in features that are smaller and taller than those of the "mosaic" brushes fabricated via SMA formation. Indeed, we observe relatively tall (up to 12 nm) and sparsely distributed clusters of grafted PS in HBC "mosaic" brushes prepared by the addition of 25% hPS (Figure 6). Here, we focus only on this system because larger fractions of hPS (50 and 75%) demonstrate very similar results. In some instances (e.g., annealed in 1,4-dioxane (Figure 6a) and thermally (Figure 6d)), P4VP domains gather in clusters or groups and have a poor distribution. Additionally, thermal annealing facilitates normal separation of P4VP blocks attracted by the surface (effect of preferential wetting).[15] Therefore, HBCs form tall "mosaic" brushes and have substantial coverage up to 68% after oven annealing. Toluene (Figure 6c) is a very weak solvent for P4VP and prevents efficient grafting to the surface. "Mosaic" brushes prepared from HBCs vapor annealed in chloroform produced the most uniform distribution of tall, single clusters. We speculate that chloroform facilitates the formation of HBCs and quaternization reactions between P4VP monomers and bromine groups on the surface.

Binary Brush of Strongly Immiscible Polymers. Table 1 depicts the fraction of surface area occupied by the PS "mosaic" brush estimated using AFM. The remaining area was used to graft the second counterpart of our BPB: PAAm. To prepare the surface of the substrate for grafting PAAm, we introduced vinyl (—CH═CH_2) functionality using the same quaternization reaction as before by substituting 2VP for the P4VP block. The use of C═C bonds for tethering and propagation of PAAm via in situ radical polymerization was shown to be effective in our recent work.[30] To the best of our knowledge, however, this is the first time that 2VP-terminated SAMs have been used for "grafting through". The polymerization was initiated in bulk by a photoinitiator. If special stencils are incorporated, photoinitiation allows for the generation of gradient or patterned brushes. In general, the method is robust and produces PAAm brushes of consistent grafting density.

We found that 20% AAm and 1% PI solutions were optimal; thus, all experiments reported here were performed at these concentrations. Successful "grafting through" of PAAm was demonstrated by the gain in the grafted amount associated with grafting of PAAm (Γ_{PAAm}) as measured by ellipsometry and BPB texture alterations visualized by AFM. The data on grafting amount and changes in CA (sessile droplet method) of BPBs upon exposure to water (θ_{H_2O}), methanol (θ_{MeOH}), and toluene (θ_{tol}) are shown in Table 1. The grafting amounts of PS and PAAm are used to calculate the total fractions of the BPB counterparts. On the other hand, CA is a convenient method to estimate the fractions of two counterparts presented on the BPB surface, as well as to demonstrate the surface reconstruction of the BPB upon immersion in different

DOI: 10.1021/am5080248
ACS Appl. Mater. Interfaces 2015, 7, 12505−12515

solvents. For the most switchable BPB, the CA ranged from 27° (mostly PAAm on top) to almost 80° (mostly PS on top) depending on the most recent solvent the brush was exposed to. For BPB constructed with "mosaic" brushes formed from neat BCP reference samples, the CA ranged between 25.8 ± 0.6° and 66.7 ± 2.1° regardless of the annealing method used.

According to the dynamic response scenario, a BPB readily switches when exposed to a selective solvent. Upon solvent exposure, the PS and PAAm sections of the binary brush respond differently depending on the selectivity of the solvent. When the PS−P4VP/PAAm system is exposed to water, the PAAm counterpart swells up to the surface−solvent interface while the PS brush collapses underneath the swollen PAAm brush, and vice versa when exposed to toluene. However, if a polymer fully covers the surface in a selective solvent and then dries, it forms an impenetrable layer and prevents inversion, which means BPB is in a metastable state. To overcome this state, methanol and a 1:1 methanol/THF mixture are used as transition solvents to allow for consistent switching between the strongly immiscible polymer brushes. Exposure of the samples to transition solvents that are weak for both counterparts allows for the collapse of the surface-dominating polymer film into separate clusters. In particular, successful switching (as recorded by CA and AFM) from a hydrophilic state (PAAm on top) was achieved by immersion of the samples in methanol and then in toluene for 1 min each. The inverse switch from a hydrophobic (PS on top) to hydrophilic state is achieved through immersion in the series of solvents binary methanol/THF → methanol → water for 1 min each. After exposure to "terminal" selective solvents (water or toluene), the samples are immediately dried with argon gas.

The textures of the dried binary brush surfaces after switching between hydrophobic-to-hydrophilic and reverse metastable states have been visualized with tapping mode AFM. The phase images support our findings and are shown here. Figures 7a−c, d−f, and g−i depict the morphological transitions of PS−P4VP/PAAm fabricated using SMA-based thermal annealing, HBC-based thermal annealing, and HBC-based, 1,4-dioxane vapor annealing, respectively, as listed in Table 1. In the hydrophobic state, PS occupies the top stratum of the BPB. On the basis of the relative flexibility of PS, its chains readily adopt the so-called "octopus micelles" conformation (Figure 7c).[31,32] We associate the nanoscopic depressions observed in the HBC samples upon toluene exposure (Figure 7f and i) with collapsed PAAm domains. To facilitate uniform switching, we ensure optimal lateral segregation of both polymer chains by transitioning to hydrophilic PAAm on top via a methanol−THF binary solvent, followed by neat methanol (Figure 7b, e, and h) and then DI water (Figure 7a, d, and g). We identify the tall domains (20−30 nm in width and 10 nm in height) populating the BPB surface as grafted PAAm after exposure to water. The orthogonal directionality of such a surface reconstruction in BPBs allows for dominant polymer brushes to push to the surface−solvent interface as discussed by Mueller et al.[9]

The reversible switching of PS−P4VP/PAAm is presented as a change in the fraction of PS that is on the top of the BPB, calculated using the Cassie−Baxter equation[33,34]

$$\cos(\theta) = \varphi_{PS} \cos(\theta_{PS}) + (1 - \varphi_{PS}) \cos(\theta_{PAAm}) \quad (1)$$

where θ, θ_{PS}, and θ_{PAAm} are the CA of the measured BPB, the neat PS brush, and the neat PAAm brush, respectively, φ_{PS} is the fraction of PS present on the surface, and $1 - \varphi_{PS}$ represents the PAAm fraction.

Figure 8 shows the change in PS fraction for PS−P4VP/PAAm when exposed to water (selective solvent for PAAm)

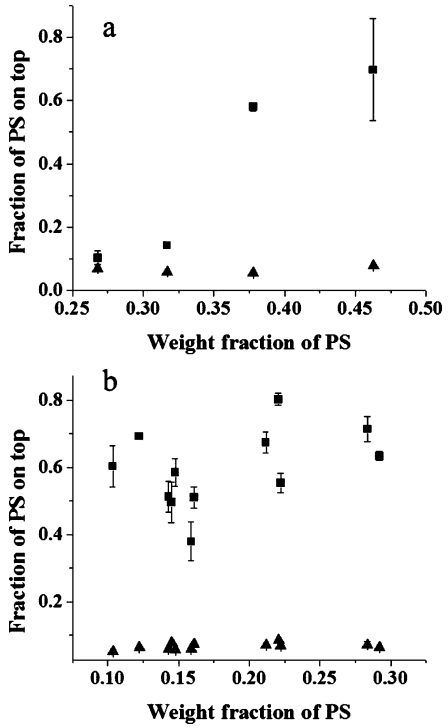

Figure 8. Fraction of PS on top for PS−P4VP/PAAm made of a "mosaic" of SMA (a) and HBC (b) as a function of PS weight fraction calculated from CA measurements after exposure to water (▲, selective for PAAm) and toluene (■, selective for PS).

and toluene (selective solvent for PS) for BPB-based on SMA and HBC "mosaic" brushes. Neat PS and PAAm brush CAs are 91 and 12°, respectively. The dominant polymer forms a glassy metastable state when dried, which would ideally result in full coverage by PS after exposure to toluene. The highest fraction of PS on top was ∼0.8 after toluene exposure. Not much change was observed in the PS fraction on top when exposured to water and then methanol (Table 1); this transition is crucial for uniform switching to PS on top after exposure to toluene. All transitions reported in Figure 8 were fully reversed at least 3 times with an accuracy that was within the standard deviation of CA measurements as represented by the error bars.

The asymmetric nature of the PS−P4VP/PAAm brushes is notable. After exposure to toluene, a binary transition solvent followed by methanol and water is required for successful switching from a hydrophobic to hydrophilic state, whereas the inverse process can occur without the use of the binary solvent, just water to neat methanol to toluene. Homogenous switching only occurs when the samples are successively exposed to the solvent sequence in wet states. As mentioned, drying between solvent sequences results in a glassy metastable state that would lead to inadequate or patchy switching.

Effective fabrication of the binary brush system was further supported using in situ force−distance measurements under deionized water after exposure to selective solvents as shown in Figure 9. For clarity, we only depict four representative approaching (green) and retracting force profiles for each PS (red) and PAAm (blue) on top, accompanied by two profiles

DOI: 10.1021/am5080248
ACS Appl. Mater. Interfaces 2015, 7, 12505−12515

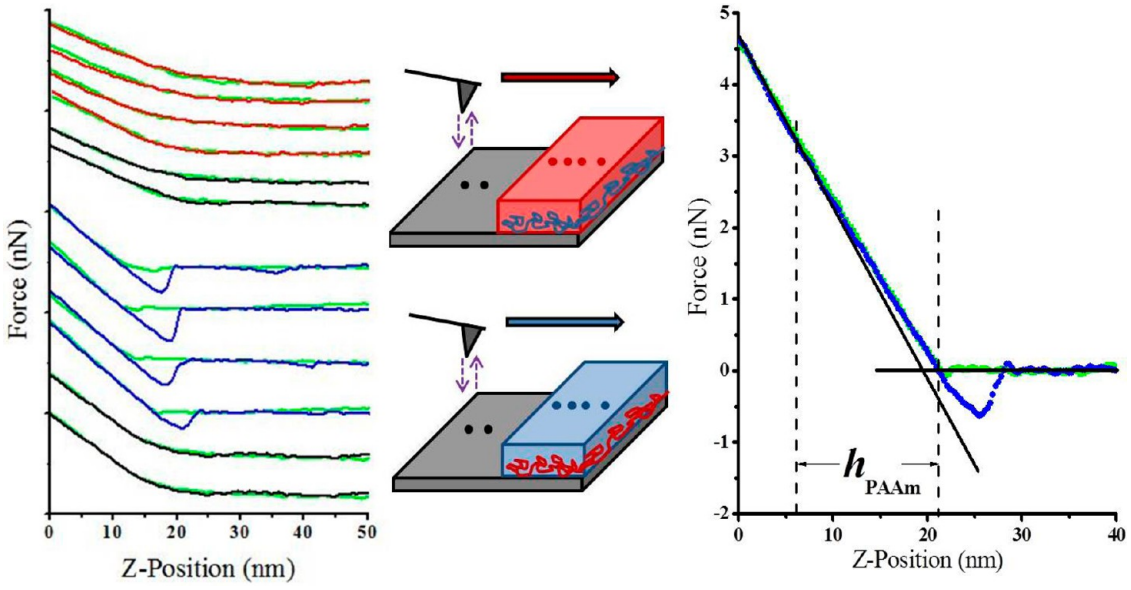

Figure 9. Sample approach (green) and retracting force profiles of a gold-coated Etalon tip during in situ AFM probe force−distance measurements under water for a scratch that exposes the Si substrate (black), and PS−P4VP/PAAm after exposure to toluene (PS on top, red) and water (PAAm on top, blue). The PS−P4VP/PAAm sample was fabricated using HBC with 25% hPS as an additive and chloroform vapor annealing as shown in Table 1.

each measured on scratches exposing the Si substrate. As stated by O'Shea et al., we assume a linear relationship between the cantilever deflection and sample displacement when the tip comes in contact with the surface.[35] Thus, the force on the tip (F) is equivalent to the cantilever deflection (D_c) multiplied by the spring constant (k), such that $F = kD_c$ according to Hooke's law.

The net force is assumed to be zero when the tip is far from the surface and begins to increase exponentially as the probe is moved closer to the surface. The tip−sample distance is referred to as zero at the point where the net force begins to increase.[35] The retracting force profiles shown in Figure 9 are for PS−P4VP/PAAm samples fabricated using "mosaics" made of HBC and chloroform vapor annealing (Table 1). All of the approach force profiles (green) were similar and showed the AFM tip experiencing an exponentially growing repulsive force at a tip−substrate distance starting at ∼20 nm. There is little to no adhesion force observed between the AFM probe and the PS layer on top or bare Si substrate, and the force profiles are fairly reversible. This means that the tip is unable to penetrate the PS layer and indent the underlying PAAm layer, similar to bare Si. After switching from PS on top to PAAm using methanol as a transition solvent, the in situ force profile of PAAm on top depicts a slight increase in attractive forces between the tip and surface until a strong repulsive force is perceived prior to retraction. During tip retraction, the presence of noncovalent adhesive interactions, such as van der Waals and capillary interactions, results in a rapid jump in the deflection signal once the pull-off force is achieved. Altogether, the full approach−retraction circle forms hysteresis typical for adhesive probe−surface interactions as discussed by Cohen et al.[36] As the tip approaches the surface, it penetrates the swollen PAAm layer by displacing PAAm's polymer chains and snaps into the sample surface. The hysteresis is a consequence of the adhesive force accredited to the cantilever tip coming into contact with the underlying PS mosaic or Si substrate. Deviations in the pull-off force value can be associated with the differences within the underlying substance (i.e., "mosaic" vs SAM surface).

Controlled Bacterial Cell Adhesion. Immersing a BPB sample with PS on top in water causes the PS layer to become a rigid, impenetrable top layer. According to our observations, this inhibits direct switching if it is exposed to water for at least 2 h. We use this feature of the PS−P4VP/PAAm brush made of HBC with 25% hPS annealed in chloroform to demonstrate the applicability of "mosaic"-based BPBs to control adhesion of bacterial cells. The sample described above was used to model bioadhesion capabilities because it demonstrated the widest range in wettability response changes. Past research has demonstrated the ability of PS to promote cell adhesion and PAAm to promote antibioadhesion properties.[37−39] Preliminary studies were conducted to observe cell adhesion using model *E. coli* microorganisms on a "mosaic" PS−P4VP/PAAm brush in comparison to a 150 nm thick PS film, a neat PS brush (3 nm thick), and a neat PAAm brush (12 nm thick) as shown in Figure 10. The optical microscope images demonstrate contrast in cell populations between reference samples and either neat PS (Figure 10b) or PAAm (Figure 10c) brushes. No significant difference is observed between the PS thick film (Figure 10a) and brush (Figure 10b). Thus, the thickness of the PS swollen layer in PS−P4VP/PAAm is sufficient to demonstrate that biofouling is independent of the potential influence of thickness.[40] Figures 10d (PS on top) and 10e (PAAm on top) depict *E. coli* adherence to the same sample that was split in two halves and respectively switched to accommodate both top brush compositions in the same cell culture for consistency. Only a few cells are seen in the optical images of the neat PAAm and PS−P4VP/PAAm (PAAm on top) brushes, which may result from cells adhering to surface defects. After the samples were air dried, the adhered *E. coli* cells were immediately scanned with AFM in the tapping mode. We observed the presence of fimbria extending from the cells deposited on PS surfaces, which indicate the positive affinity of the cells toward PS.[41,42] The few cells observed on PAAm

DOI: 10.1021/am5080248
ACS Appl. Mater. Interfaces 2015, 7, 12505−12515

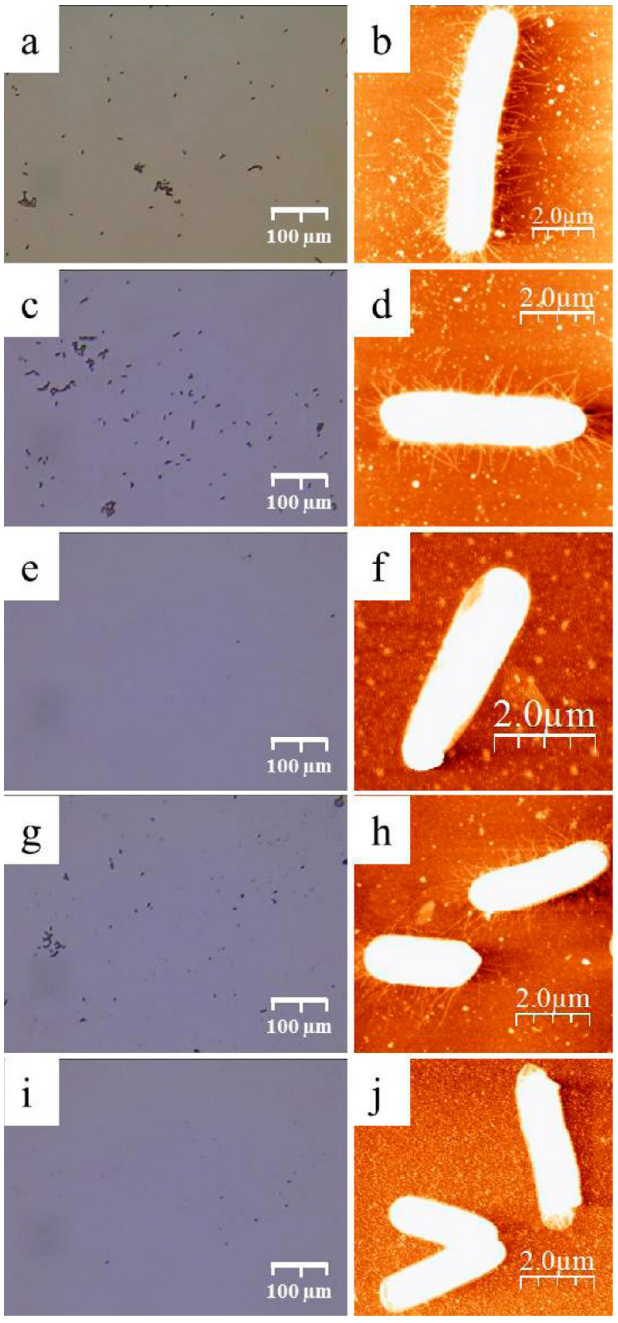

Figure 10. Optical microscope images and AFM topography scans of *E. coli* on a (a, b) 150 nm thick neat PS film, (c, d) 3 nm thick relaxed PS−P4VP brush, (e, f) 12 nm thick neat PAAm brush, and PS−P4VP/PAAm with (g, h) PS or (i, j) PAAm on top, respectively.

surfaces did not have such fimbria. These bacterial cell adhesion experiments were limited by incubation time (2 h) because longer incubations could have sporadic, patchy switching of the BPB with PS on top to the hydrophilic state. The results of this initial *E. coli* model provide a perspective for better reversible control (fouling−antifouling) in cell-mediated applications, such as cell detachment and bacterial biofilm inhibition, which would be beneficial for the medical, water treatment, and food industries.[43,44]

CONCLUSION

In this work, we employed the phenomenon of microphase separation observed in SMAs and HBCs to produce polymer brushes with nanoscopic patterns, which we termed "mosaic" brushes. PS−P4VP BCP is the building material of these brushes. Once deposited on a bromine-terminated SAM, a chemical reaction between the SAM and P4VP units of the BCP tethers the PS chain assemblies in patches. The low molecular weight additive distributed in domains of the minor reactive block of P4VP facilitates the formation of SMA cylinder morphologies. It produces wide (20−30 nm) and low profile (5−6 nm in height) patches of a PS "mosaic" brush. Contrarily, the homopolymer hPS added to PS−P4VP is solubilized in the major phase of PS, thus resulting in taller (up to 12 nm) and more compact grafted PS clusters produced from HBCs. This is only a general trend and the effect of the annealing method (thermal or solvent vapors) has a significant impact on the morphology/distribution of the "mosaic" brush. During annealing, segmental mobility concurrently facilitates two processes: improving the order of the assemblies and the quaternization reaction on the interface with the SAM. In both the HBC and SMA cases, the "mosaic" brushes are homogeneously distributed over the entire sample area and are fairly uniform in size.

The use of such "mosaic" brushes is an attractive platform for secondary grafting to form binary polymer brushes with highly contrasting responses. The formation of well-defined nanoscopic clusters of grafted PS opens the surface for further modifications. We successfully introduced vinyl groups —C═C onto the substrate surface by quaternization reactions between 2VP monomers and the bromine-terminated SAM. This allowed us to attach chains of PAAm by a "grafting through" approach. In this manner, two strongly immiscible polymers (i.e., polymers with no common solvents) were tethered together on the same substrate. Depending on the polymeric counterpart that occupies the top stratum, two distinctly different states with specific properties and morphologies are observed for the PS−P4VP/PAAm BPBs: (i) a hydrophobic state (PS on top) with low adhesion to an AFM probe and (ii) a hydrophilic state (PAAm on top) in which AFM probe adhesion to a swollen PAAm brush in water is significant. The adhesion of bacterial cells to a BPB in these two states also shows strong contrast. *E. coli* cells stick to the BPB when PS occupies the brush surface and slide off the BPB when PAAm is on top. The implications of block copolymer assemblies to produce nanopatterned polymer brushes open new perspectives on high constrast responsive surfaces that will find numerous applications in biomaterials, water and food treatment, packaging, sensorics, microfluidics, and other fields of fine engineering.

AUTHOR INFORMATION

Corresponding Author

*E-mail: a.sidorenko@usciences.edu. Phone: (215) 596 8836.

Notes

The authors declare no competing financial interest.

ACKNOWLEDGMENTS

This work was funded by National Science Foundation (DMR 0947897) and in part by the Center for Drug Design and Delivery (KISK grant of the Department of Community and Economic Development, Commonwealth of Pennsylvania).

DOI: 10.1021/am5080248
ACS Appl. Mater. Interfaces 2015, 7, 12505−12515

REFERENCES

(1) Sidorenko, A.; Krupenkin, T.; Taylor, A.; Fratzl, P.; Aizenberg, J. Reversible Switching of Hydrogel-Actuated Nanostructures into Complex Micropatterns. *Science* **2007**, *315* (5811), 487−490.

(2) Sidorenko, A.; Krupenkin, T.; Aizenberg, J. Controlled Switching of the Wetting Behavior of Biomimetic Surfaces with Hydrogel-Supported Nanostructures. *J. Mater. Chem.* **2008**, *18* (32), 3841−3846.

(3) Sidorenko, A.; Minko, S.; Schenk-Meuser, K.; Duschner, H.; Stamm, M. Switching of Polymer Brushes. *Langmuir* **1999**, *15* (24), 8349−8355.

(4) Lemieux, M.; Usov, D.; Minko, S.; Stamm, M.; Shulha, H.; Tsukruk, V. V. Reorganization of Binary Polymer Brushes: Reversible Switching of Surface Microstructures and Nanomechanical Properties. *Macromolecules* **2003**, *36* (19), 7244−7255.

(5) Vyas, M. K.; Schneider, K.; Nandan, B.; Stamm, M. Switching of Friction by Binary Polymer Brushes. *Soft Matter* **2008**, *4* (5), 1024−1032.6.

(6) Ionov, L.; Minko, S. Mixed Polymer Brushes with Locking Switching. *ACS Appl. Mater. Interfaces* **2012**, *4* (1), 483−489.

(7) Tsyalkovsky, V.; Burtovyy, R.; Klep, V.; Lupitskyy, R.; Motornov, M.; Minko, S.; Luzinov, I. Fluorescent Nanoparticles Stabilized by Poly(ethylene glycol) Containing Shell for pH-Triggered Tunable Aggregation in Aqueous Environment. *Langmuir* **2010**, *26* (13), 10684−92.

(8) Minko, S.; Patil, S.; Datsyuk, V.; Simon, F.; Eichhorn, K.-J.; Motornov, M.; Usov, D.; Tokarev, I.; Stamm, M. Synthesis of Adaptive Polymer Brushes via "Grafting To" Approach from Melt. *Langmuir* **2002**, *18* (1), 289−296.

(9) Minko, S.; Muller, M.; Usov, D.; Scholl, A.; Froeck, C.; Stamm, M. Lateral versus Perpendicular Segregation in Mixed Polymer Brushes. *Phys. Rev. Lett.* **2002**, *88* (3), 035502/1−035502/4.

(10) Usov, D.; Gruzdev, V.; Nitschke, M.; Stamm, M.; Hoy, O.; Luzinov, I.; Tokarev, I.; Minko, S. Three-Dimensional Analysis of Switching Mechanism of Mixed Polymer Brushes. *Macromolecules* **2007**, *40* (24), 8774−8783.

(11) Bates, F. S.; Fredrickson, G. H. Block Copolymer Thermodynamics: Theory and Experiment. *Annu. Rev. Phys. Chem.* **1990**, *41*, 525−557.

(12) Leibler, L. Theory of Microphase Separation in Block Copolymers. *Macromolecules* **1980**, *13* (6), 1602−1617.

(13) Sidorenko, A.; Tokarev, I.; Minko, S.; Stamm, M. Ordered Reactive Nanomembranes/Nanotemplates from Thin Films of Block Copolymer Supramolecular Assembly. *J. Am. Chem. Soc.* **2003**, *125* (40), 12211−12216.

(14) Tokarev, I.; Krenek, R.; Burkov, Y.; Schmeisser, D.; Sidorenko, A.; Minko, S.; Stamm, M. Microphase Separation in Thin Films of Poly(styrene-block-4-vinylpyridine) Copolymer-2-(4′-hydroxybenzeneazo)benzoic Acid Assembly. *Macromolecules* **2005**, *38* (2), 507−516.

(15) Jeong, U.; Kim, H.-C.; Rodriguez, R. L.; Tsai, I. Y.; Stafford, C. M.; Kim, J. K.; Hawker, C. J.; Russell, T. P. Asymmetric Block Copolymers with Homopolymers: Routes to Multiple Length Scale Nanostructures. *Adv. Mater.* **2002**, *14* (4), 274−276.

(16) Kim, S. H.; Misner, M. J.; Russell, T. P. Solvent-Induced Ordering in Thin Film Diblock Copolymer/Homopolymer Mixtures. *Adv. Mater.* **2004**, *16* (23−24), 2119−2123.

(17) Roland, S.; Pellerin, C.; Bazuin, C. G.; Prud'homme, R. E. Evolution of Small Molecule Content and Morphology with Dip-Coating Rate in Supramolecular PS−P4VP Thin Films. *Macromolecules* **2012**, *45* (19), 7964−7972.

(18) Kuila, B. K.; Stamm, M. Supramolecular Complex of Poly(styrene)-*b*-poly(4-vinylpyridine) and 1-Pyrenebutyric Acid in Thin Film. *Macromol. Symp.* **2011**, *303*, 85−94.

(19) Hagaman, D.; Gredzik, J.; Peart, P. A.; McCaffery, J. M.; Tovar, J. D.; Sidorenko, A. Block Copolymer Supramolecular Assembly Using a Precursor to a Novel Conjugated Polymer. *Polym. Chem.* **2013**, *4* (5), 1482−1490.

(20) Hagaman, D.; Enright, T. P.; Sidorenko, A. Block Copolymer Supramolecular Assembly beyond Hydrogen Bonding. *Macromolecules* **2012**, *45* (1), 275−282.

(21) Stuen, K. O.; Detcheverry, F. A.; Craig, G. S. W.; Thomas, C. S.; Farrell, R. A.; Morris, M. A.; de Pablo, J. J.; Nealey, P. F. Graphoepitaxial Assembly of Asymmetric Ternary Blends of Block Copolymers and Homopolymers. *Nanotechnology* **2010**, *21* (49), 495301.

(22) Stoykovich, M. P.; Edwards, E. W.; Solak, H. H.; Nealey, P. F. Phase Behavior of Symmetric Ternary Block Copolymer-Homopolymer Blends in Thin Films and on Chemically Patterned Surfaces. *Phys. Rev. Lett.* **2006**, *97* (14), 147802/1−147802/4.

(23) Winey, K. I.; Thomas, E. L.; Fetters, L. J. Swelling of Lamellar Diblock Copolymer by Homopolymer: Influences of Homopolymer Concentration and Molecular Weight. *Macromolecules* **1991**, *24* (23), 6182−6188.

(24) Stuen, K. O.; Thomas, C. S.; Liu, G.; Ferrier, N.; Nealey, P. F. Dimensional Scaling of Cylinders in Thin Films of Block Copolymer-Homopolymer Ternary Blends. *Macromolecules* **2009**, *42* (14), 5139−5145.

(25) Chevalier, X.; Nicolet, C.; Tiron, R.; Gharbi, A.; Argoud, M.; Couderc, C.; Fleury, G.; Hadziioannou, G.; Iliopoulos, I.; Navarro, C. Improvements of Self-Assembly Properties via Homopolymer Addition or Block-Copolymer Blends. *Proc. SPIE* **2014**, *9049* (Alternative Lithographic Technologies VI), 90490T/1−90490T/13.

(26) Enright, T. P.; Hagaman, D.; Kokoruz, M.; Coleman, N.; Sidorenko, A. Gradient and Patterned Polymer Brushes by Photo-initiated "Grafting Through" Approach. *J. Polym. Sci., Part B: Polym. Phys.* **2010**, *48* (14), 1616−1622.

(27) Motschmann, H.; Stamm, M.; Toprakcioglu, C. Adsorption Kinetics of Block Copolymers from a Good Solvent: A Two-Stage Process. *Macromolecules* **1991**, *24* (12), 3681−3688.

(28) Horcas, I.; Fernandez, R.; Gomez-Rodriguez, J. M.; Colchero, J.; Gomez-Herrero, J.; Baro, A. M. WSXM: A Software for Scanning Probe Microscopy and a Tool for Nanotechnology. *Rev. Sci. Instrum.* **2007**, *78* (1), 013705/1−013705/8.

(29) Cunliffe, D.; Smart, C. A.; Alexander, C.; Vulfson, E. N. Bacterial Adhesion at Synthetic Surfaces. *Appl. Environ. Microbiol.* **1999**, *65* (11), 4995−5002.

(30) Chu, E.; Sidorenko, A. Surface Reconstruction by a "Grafting Through" Approach: Polyacrylamide Grafted onto Chitosan Film. *Langmuir* **2013**, *29* (40), 12585−12592.

(31) Horiuchi, S.; Nakagawa, A.; Liao, Y.; Ougizawa, T. Interfacial Entanglements between Glassy Polymers Investigated by Nano-fractography with High-Resolution Scanning Electron Microscopy. *Macromolecules* **2008**, *41* (21), 8063−8071.

(32) Jentzsch, C.; Sommer, J.-U. Polymer Brushes in Explicit Poor Solvents Studied Using a New Variant of the Bond Fluctuation Model. *J. Chem. Phys.* **2014**, *141* (10), 104908/1−104908/10.

(33) Cassie, A. B. D.; Baxter, S. Wettability of Porous Surfaces. *Trans. Faraday Soc.* **1944**, *40*, 546−551.

(34) Cassie, A. B. D. Contact Angles. *Discuss. Faraday Soc.* **1948**, *3*, 11−16.

(35) O'Shea, S. J.; Welland, M. E.; Rayment, T. An Atomic Force Microscope Study of Grafted Polymers on Mica. *Langmuir* **1993**, *9* (7), 1826−1835.

(36) Cohen, S. R.; Kalfon-Cohen, E. Dynamic Nanoindentation by Instrumented Nanoindentation and Force Microscopy: A Comparative Review. *Beilstein J. Nanotechnol.* **2013**, *4*, 815−833.

(37) Cringus-Fundeanu, I.; Luijten, J.; van der Mei, H. C.; Busscher, H. J.; Schouten, A. J. Synthesis and Characterization of Surface-Grafted Polyacrylamide Brushes and Their Inhibition of Microbial Adhesion. *Langmuir* **2007**, *23* (9), 5120−5126.

(38) Fundeanu, I.; Klee, D.; Schouten, A. J.; Busscher, H. J.; van der Mei, H. C. Solvent-Free Functionalization of Silicone Rubber and Efficacy of PAAm Brushes Grafted from an Amino-PPX Layer Against Bacterial Adhesion. *Acta Biomater.* **2010**, *6* (11), 4271−4276.

(39) Fundeanu, I.; van der Mei, H. C.; Schouten, A. J.; Busscher, H. J. Microbial Adhesion to Surface-Grafted Polyacrylamide Brushes After

DOI: 10.1021/am5080248
ACS Appl. Mater. Interfaces 2015, 7, 12505−12515

Long-Term Exposure to PBS and Reconstituted Freeze-Dried Saliva. *J. Biomed. Mater. Res., Part A* **2010**, *94A* (3), 997−1000.
(40) Ren, T.; Mao, Z.; Guo, J.; Gao, C. Directional Migration of Vascular Smooth Muscle Cells Guided by a Molecule Weight Gradient of Poly(2-hydroxyethyl methacrylate) Brushes. *Langmuir* **2013**, *29* (21), 6386−6395.
(41) Castonguay, M.-H.; van der Schaaf, S.; Koester, W.; Krooneman, J.; van der Meer, W.; Harmsen, H.; Landini, P. Biofilm Formation by *Escherichia coli* is Stimulated by Synergistic Interactions and Co-Adhesion Mechanisms with Adherence-Proficient Bacteria. *Res. Microbiol.* **2006**, *157* (5), 471−478.
(42) Schembri, M. A.; Christiansen, G.; Klemm, P. FimH-Mediated Autoaggregation of *Escherichia coli*. *Mol. Microbiol.* **2001**, *41* (6), 1419−1430.
(43) Morton, L. H. G.; Surman, S. B. Biofilms in Biodeterioration - A Review. *Int. Biodeterior. Biodegrad.* **1995**, *34* (3/4), 203−221.
(44) Bower, C. K.; McGuire, J.; Daeschel, M. A. The Adhesion and Detachment of Bacteria and Spores on Food-Contact Surfaces. *Trends Food Sci. Technol.* **1996**, *7* (5), 152−157.

DOI: 10.1021/am5080248
ACS Appl. Mater. Interfaces 2015, 7, 12505−12515